JOURNAL OF ELECTROMAGNETIC ENGINEERING AND SCIENCE, VOL. 24, NO. 2, 170~177, MAR. 2024

https://doi.org/10.26866/jees.2024.2.r.217
ISSN 2671-7263 (Online) · ISSN 2671-7255 (Print)

Robust Ku-Band GaN Low-Noise Amplifier MMIC

Seong-Hee Han · Dong-Wook Kim*

Abstract

This paper employs the 0.2 μm ETRI GaN HEMT process on SiC to develop a Ku-band GaN low-noise amplifier monolithic microwave integrated circuit (MMIC) characterized by high-input power robustness for radar transceiver modules. A source degeneration inductor is employed to obtain the proposed amplifier's stable operation and the compromised impedance trajectory of the maximum available gain and minimum noise figure. The analysis results show simultaneous gain and noise impedance matching, achieved using only a small number of passive elements. Furthermore, the proposed low-noise amplifier MMIC secures a linear gain of 21.3–22.6 dB, an input return loss of 19.6–21.4 dB, and a noise figure of 1.7–1.8 dB in the 15–16 GHz frequency range. It also exhibits an input 1 dB compression point of 0.4–1.5 dBm in the single-tone power test, and an input third-order intercept point of 5.8–10.1 dBm within the 15–16 GHz frequency range in the two-tone intermodulation distortion test.

Key Words: GaN, HEMT, Ku-Band, Low-Noise Amplifier, MMIC, Source Degeneration.

I. Introduction

Microwave low-noise amplifiers are widely used in transceiver modules for military and civilian radar and communication systems. Notably, low-noise amplifiers in military systems must withstand high power and possess low-noise characteristics over a wide frequency range. To meet these requirements, low-noise amplifiers using GaN high electron mobility transistors (HEMTs) on SiC, which have a higher breakdown voltage, higher electron velocity, and better thermal conductivity than Si or GaAs devices, have been extensively researched [1, 2]. While GaAs pseudomorphic HEMTs (pHEMTs), characterized by low operating voltage, high electron mobility, and high maximum operating frequency, are actively used in transceiver modules, they require the application of additional limiters to block leaked power from the transmitter and to protect the receiver circuit from unwanted high-input power, which adversely affects both the size reduction of the module and the necessary low-noise performance. This drawback has contributed to a recent research trend focused on using GaN HEMTs on SiC in the receiver module [3–8].

This study designs and fabricates a GaN low-noise amplifier monolithic microwave integrated circuit (MMIC) for a Ku-band RF transceiver module. To achieve this, a 0.2 μm GaN HEMT on SiC obtained from the Electronics and Telecommunications Research Institute (ETRI) was utilized, while the transistor was stabilized using the source feedback technique by adding an inductor to the source of the transistor. This allowed for a favorable impedance trajectory marked by high-gain matching and low-noise matching [9, 10]. However, while the source inductance improved the stability of the transistor, it also degraded the available gain and noise figure. As a result, this study chose to focus on the optimal inductance for the target frequency region to minimize gain reduction and alleviate the difficulty involved in impedance matching. Therefore, this paper presents the design and measurement results of a Ku-band, highly robust GaN low-noise amplifier MMIC equipped with a

Manuscript received March 10, 2023 ; Revised July 03, 2023 ; Accepted October 18, 2023. (ID No. 20230310-052J)
Department of Radio and Information Communications Engineering, Chungnam National University, Daejeon, Korea.
*Corresponding Author: Dong-Wook Kim (e-mail: dwkim21c@cnu.ac.kr)

source feedback inductance fabricated using the 0.2 μm GaN HEMT process presented by ETRI.

II. Circuit Design

1. The 0.2 μm GaN HEMT

The GaN HEMT on SiC utilized in this study featured a gate length of 0.2 μm, and a gate width of 4 μm × 50 μm, and could operate up to 26 GHz. Considering the bias conditions of V_{DS} = 20 V and I_{DS} = 20 mA, the maximum available gain (MAG) and minimum noise figure at 50 Ω in the Ku-band (15–16 GHz) of the destabilized transistor were expected to be 12.41–12.67 dB and 1.85–1.99 dB, respectively. The extrapolated transistor cutoff frequency f_T and maximum oscillation frequency f_{max} at the bias point were 31.7 GHz and 70.3 GHz, respectively. Furthermore, the 2 μm × 100 μm test transistor used for process control monitoring had a breakdown voltage of more than 170 V and a maximum gate-to-source voltage of 0 V.

For low-noise amplification, the 4 μm × 50 μm and 4 μm × 100 μm GaN HEMTs were available from ETRI. Since the former offered a better noise figure by about 0.2 dB in the Ku-band than the latter, the 4 μm × 50 μm transistor was chosen as the amplifying device in this study, despite the 2 dB MAG reduction.

The design specifications of the proposed low-noise amplifier MMIC had to ensure attaining a linear gain of 15 dB or more and a noise figure of 2.8 dB or less, as shown in Table 1. Notably, the capacitor in the circuit design was replaced with an equivalent circuit model extracted from the measured data, while the inductor and other matching elements were modeled using Keysight ADS 2.5D electromagnetic momentum simulations.

The *S*-parameter data at V_{DS} = 20 V and I_{DS} = 20 mA indicated that the transistor was unstable in the Ku-band. Before proceeding with the gain and noise simulation, the stable operation of the transistor had to be secured. Therefore, for transistor stabilization, an inductive component was added to the source of the transistor by inserting a microstrip line between the transistor source and the ground, as shown in Fig. 1. Notably, a microstrip line inductor was utilized, as it was found to be more effective in the Ku-band than loop or spiral inductors with regard to self-resonance and size reduction.

Fig. 2 depicts the variations in the MAG, the noise figure at 50 Ω, and the stability factor (K), while Fig. 3 presents the changes in the input/output reflection coefficients and optimal noise impedance in the Ku-band with an increase in the source inductance up to 1.5 nH. It is evident that with an increase in source inductance in the Ku-band, the stability factor K improved, but the noise figure at 50 Ω decreased, owing to the fact that the optimum noise source impedance had approached 50 Ω. The MAG was observed to be slightly reduced as well. This indicates that with proper source inductance, an impedance trajectory that balances the overall performance of stability, gain, and noise figure while minimizing the required number of passive elements in the matching circuit can be obtained. In this study, the microstrip lines used in all three stages of the designed

Table 1. Design specifications of the Ku-band GaN low-noise amplifier MMIC

Parameter	Value (mm)
Frequency (GHz)	15−16
Linear gain (dB)	≥15
Noise figure (dB)	≤2.8
Input return loss (dB)	≥10
Size (mm^2)	1.66 × 1.16

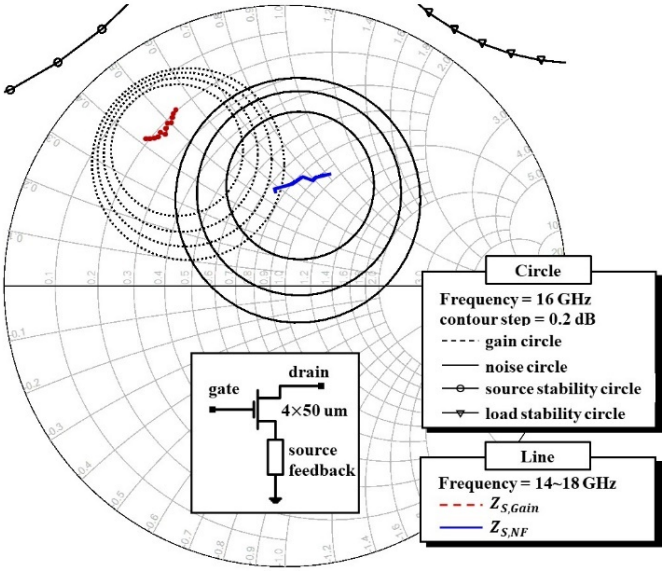

Fig. 1. The impedance trajectories of the optimal gain and minimum noise figure of the 4 × 50 μm transistor with 1.4 nH source feedback.

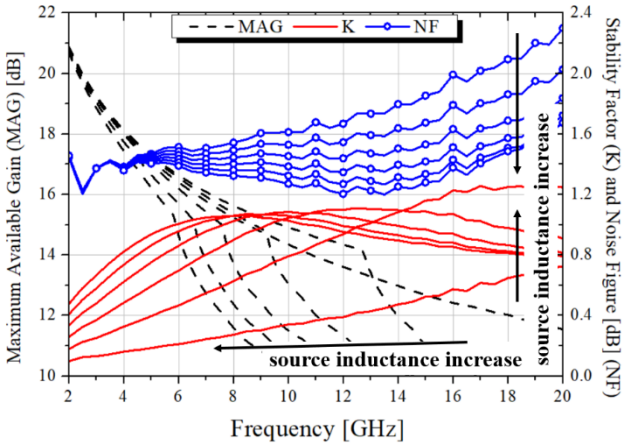

Fig. 2. Variation in the maximum available gain (MAG), noise figure (NF) at 50 Ω, and stability factor (K) of the 4 × 50 μm transistor with an increase in the source inductance up to 1.5 nH (bias conditions: V_{DS} = 20 V and I_{DS} = 20 mA).

amplifier had a line width of 25 μm and a length of 200 μm, which is equivalent to an inductance of approximately 1.4 nH, including a via-hole inductance.

2. Matching Circuit

Fig. 1 illustrates the gain circle and noise circle at 16 GHz, including the impedance trajectories for the optimal gain and minimum noise figure between the 14–18 GHz frequency band, on inserting the microstrip line into the transistor source.

The optimal gain impedance ($Z_{S,Gain}$) and noise source impedance ($Z_{S,NF}$) at 16 GHz were 11.51 + *j*23.09 Ω and 40.72 + *j*37.50 Ω, respectively. The corresponding gain and noise figure achieved with $Z_{S,Gain}$ were 9.66 dB and 2.37 dB, while those achieved with $Z_{S,NF}$ were 8.18 dB and 1.37 dB, respectively. Subsequently, the compromised optimal source impedance ($Z_{S,OPT}$ = 20.3 + *j*26.4 Ω) and load impedance ($Z_{L,OPT}$ = 36.0 + *j*74.8 Ω) were selected to balance the gain and noise figure. The expected gain and noise figure at these impedance conditions were approximately 9.4 dB and 1.7 dB, respectively.

To obtain a high gain, the proposed Ku-band low-noise amplifier was designed based on a three-stage cascaded common-source configuration, the schematic circuit diagram for which is depicted in Fig. 4. The same bias conditions were applied to each stage, while a gate bias voltage was shared through 250 Ω gate resistors and bypass capacitors to ensure stability. Furthermore, RF choke inductors and resistor-capacitor shunt trap circuits were inserted into the drain bias circuit to suppress low-frequency oscillation, and 2.5 Ω series resistors were employed to connect the drain bias and prevent additional loop feedback [10, 11].

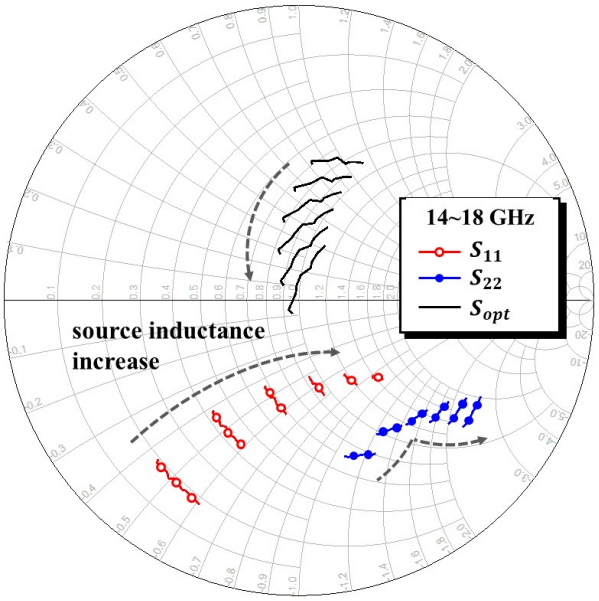

Fig. 3. Variations in the input, output, and optimum noise impedance trajectories of the 4 × 50 μm transistor with an increase in the source inductance up to 1.5 nH (bias conditions: V_{DS} = 20 V and I_{DS} = 20 mA).

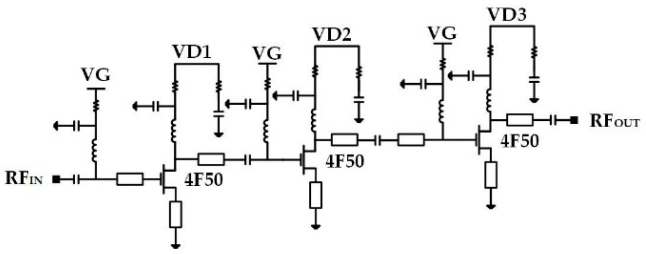

Fig. 4. Schematic circuit diagram of the proposed Ku-band low-noise amplifier.

Fig. 5 shows the impedance trajectories of the input, output, and inter-stage matching circuits on a Smith chart. The input and output matching circuits managed to move the complex conjugate source impedance ($Z_{S,OPT,1}^*$) of the first-stage transistor to 50 Ω and the complex conjugate load impedance ($Z_{L,OPT,3}^*$) of the third-stage transistor to 50 Ω, respectively. Subsequently, when the input matching circuit was connected to the first-stage transistor, the inter-stage matching circuit between the first and second stages moved the output impedance ($Z_{OUT,1}$) of the first transistor to the complex source impedance ($Z_{S,OPT,2}$) of the second-stage transistor. Furthermore, when the input matching circuit and inter-stage matching circuit between the first and second stages were applied to each stage, the inter-stage matching circuit between the second and third stages moved the output impedance ($Z_{OUT,2}$) of the second transistor to the complex source impedance ($Z_{S,OPT,3}$) of the third-stage transistor. Finally, the matching circuit design was completed by fine-tuning the circuit performance.

Fig. 6 shows a photograph of the fabricated Ku-band GaN HEMT low-noise amplifier MMIC, which occupied an area of 1.66 mm × 1.16 mm. The MMIC chip was attached to an aluminum carrier using a silver epoxy process for on-wafer measurement.

III. Measurement

Figs. 7 and 8 display the *S*-parameter and noise measurement results of the low-noise amplifier MMIC under the bias conditions of V_{DS} = 20 V and I_{DS} = 84 mA, respectively. The *S*-parameter measurement was performed using the cascade on-wafer probe system and the Keysight network analyzer (N5230A). Meanwhile, for noise measurement, the noise source (N4002A) and Keysight signal analyzer (N9030B) were employed. The input return loss S_{11} was measured to be 19.6–21 dB and the output return loss S_{22} was 9–12 dB in the frequency range of 15–16 GHz. Compared to the simulation results in the target frequency band, S_{11} exhibited an improvement of about 5 dB while S_{22} degraded by about 10 dB. The gain in the target frequency band was 21.3–22.6 dB, indicating a 1-dB reduction in gain on using the proposed amplifier MMIC, while the noise figure was 1.7–1.8 dB, which was a 0.4 dB improvement over the simulated results.

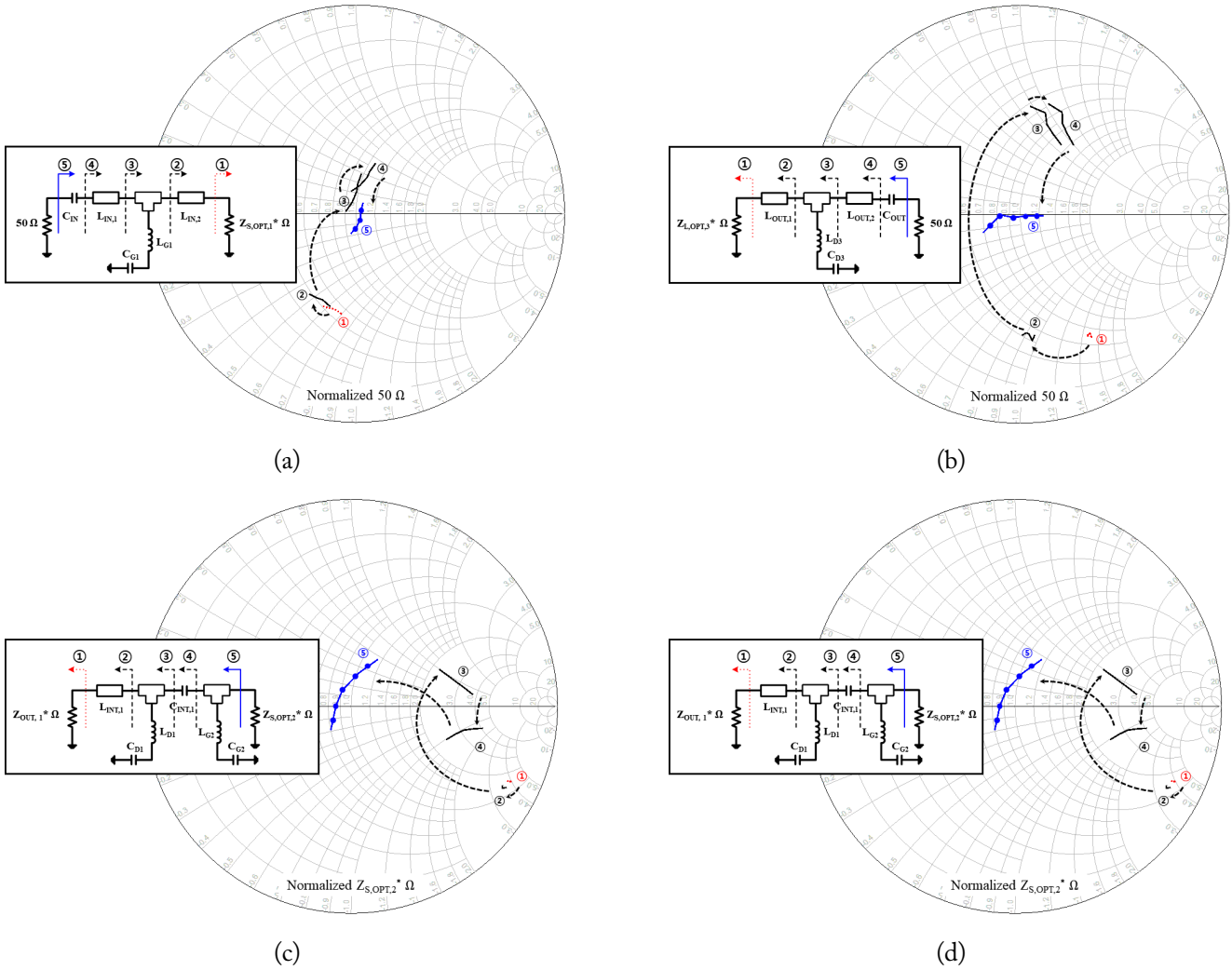

Fig. 5. Impedance trajectories of input, output, and inter-stage matching circuits (frequency range: 14.5–16.5 GHz). (a, b) Input and output matching impedance trajectory. (c) Inter-stage matching impedance trajectory between the first and second stages. (d) Inter-stage matching impedance trajectory between the second and third stages.

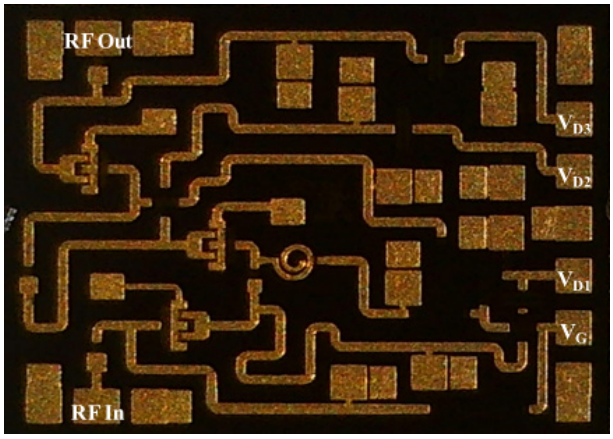

Fig. 6. The fabricated Ku-band low-noise amplifier MMIC.

Fig. 9 shows the measurement analysis results of the Ku-band low-noise amplifier MMIC. The circles in the figure represent the gain circles for a contour step of 0.1 dB and noise circles for a contour step of 0.2 dB in the 4 × 50 μm transistor at 16 GHz. The figure is an enlarged version of Fig. 1, with the designed input matching impedance ($Z_{IN,TR1,SIMUL}$*) and estimated input matching impedance ($Z_{IN,TR1,MEAS}$*) obtained from the measurement of the first-stage transistor simultaneously plotted on it. To explain the difference between the designed and estimated input matching impedance results, a capacitance change of about 10% was assumed due to the process variation, while the 2.5D electromagnetic simulation results were considered for other passive components. Furthermore, owing to an increase in the primary capacitance of the equivalent capacitor model, the debugging impedance trajectory ($Z_{IN,TR1,DEBUG}$*) was found to be similar to the actual measured results. At an impedance of $Z_{IN,TR1,DEBUG}$*, the gain degraded by about 0.8 dB and the noise figure improved by about 0.4 dB. Notably, the discrepancy between the simulated and measured results can be partly explained by variations in the dielectric deposition process that result in an impedance shift toward a region of better noise and poorer gain.

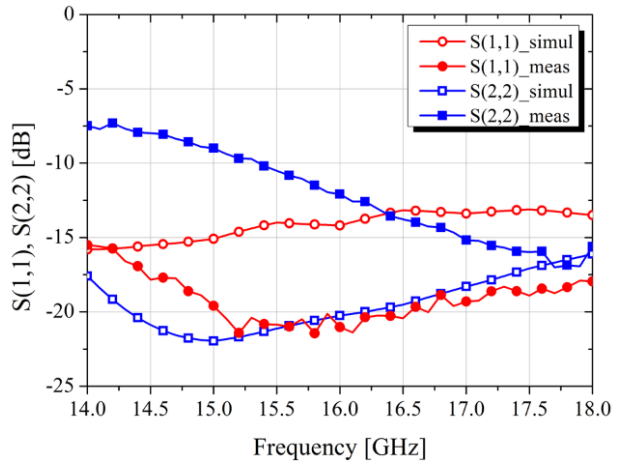

Fig. 7. Comparison of the simulated and measured *S*-parameter results.

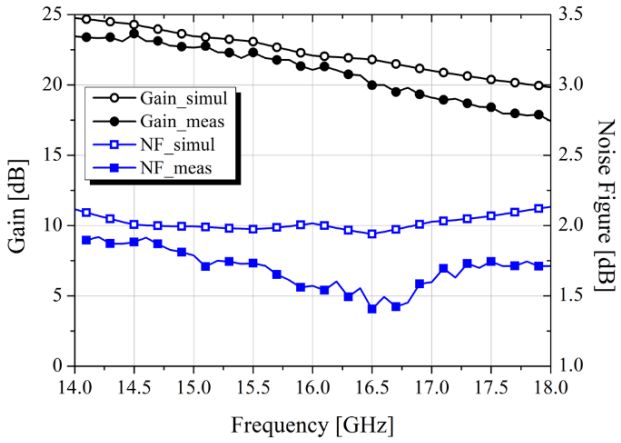

Fig. 8. Comparison of the simulated and measured gain and noise figure.

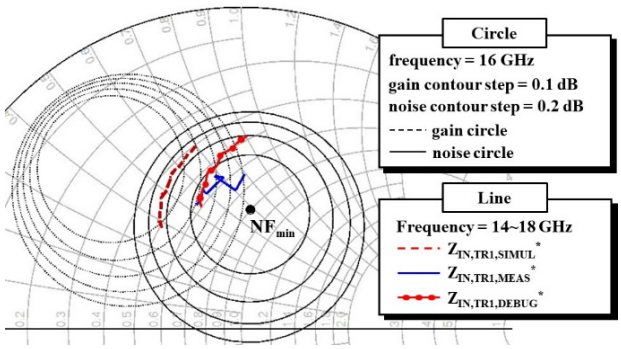

Fig. 9. Measurement analysis results of the Ku-band low-noise amplifier MMIC.

Fig. 10 presents changes in output power and power gain as functions of the input power at 15, 15.5, and 16 GHz under bias conditions of V_{DS} = 20 V and I_{DS} = 84 mA. At 15 GHz, the output 1-dB compression point (P_{1dB}) was measured to be 24.3 dBm at an input power of 1.5 dBm. Furthermore, according to the results of a full power test, the fabricated amplifier could endure an input power of about 7 dBm, which corresponds to an approximate compression point of 4.5 dB. However, when the input power exceeded 7 dBm, the power test identified the occurrence of gain degradation. Notably, the power-handling capability of the proposed amplifier could be improved to some extent by increasing the device size in the final amplifying stage. Fig. 11 depicts the measured results of the third-order intermodulation distortion product (IMD_3) at 15, 15.5, and 16 GHz when two-tone signals with a frequency interval of 50 MHz were applied to the proposed low-noise amplifier MMIC [12]. The input third-order intercept point (IIP_3), estimated from the IMD_3 component with f_{Low} = 15.05 GHz, f_{High} = 15.1 GHz, and $2f_{Low} - f_{High}$ = 15 GHz, was 8.1 dBm, while the output third-order intercept point (OIP_3) was 33.3 dBm.

Table 2 lists the measured P_{1dB}, power gain, and IIP_3 characteristics of the low-noise amplifier MMIC within the 15–16 GHz frequency range, with the output P_{1dB} being more than 20 dBm and IIP_3 measured at 5.8–10.1 dBm. Table 3 compares the results of this study with those of other published low-noise amplifier MMICs using GaAs or GaN HEMTs, establishing that the fabricated Ku-band GaN HEMT low-noise amplifier MMIC delivers excellent performance in terms of noise, circuit compactness, and power robustness [13–20].

IV. Conclusion

This study designed, fabricated, and evaluated a Ku-band GaN low-noise amplifier MMIC using ETRI's 0.2 μm GaN HEMT on SiC process. A source degeneration inductance was inserted into the transistor to induce the feedback effect required to improve stability and optimize the design impedance. It also allowed for the use of simple matching circuits and minimized chip size. The fabricated low-noise amplifier MMIC exhibited a linear gain of 21.3–22.6 dB, a noise figure of 1.7–1.8 dB, an input return loss of 19.6–21 dB, an output P1dB of more than 20 dBm, and an output IP3 of approximately 27.6–33.3 dBm in the 15–16 GHz frequency range. Th ese results indicate that the low-noise amplifier MMIC proposed in this work has the potential to play a pivotal role in the development of Ku-band military radar transceiver modules that simultaneously require high-input power endurance and low-noise performance.

This work was supported by the National Research Council of Science and Technology (NST) grant by the Korean government (MSIT) (No. CRC-19-02-ETRI).

Table 2. Measured results of the input and output P_{1dB}, power gain, and input IP_3 in terms of frequency

	$P_{1dB,in}$ (dBm)	$P_{1dB,out}$ (dBm)	Gain (dB)	IIP_3 (dBm)
15 GHz	1.5	24.3	23.3	10.1
15.5 GHz	1.0	21.9	21.8	5.8
16 GHz	0.4	20.2	20.7	7.6

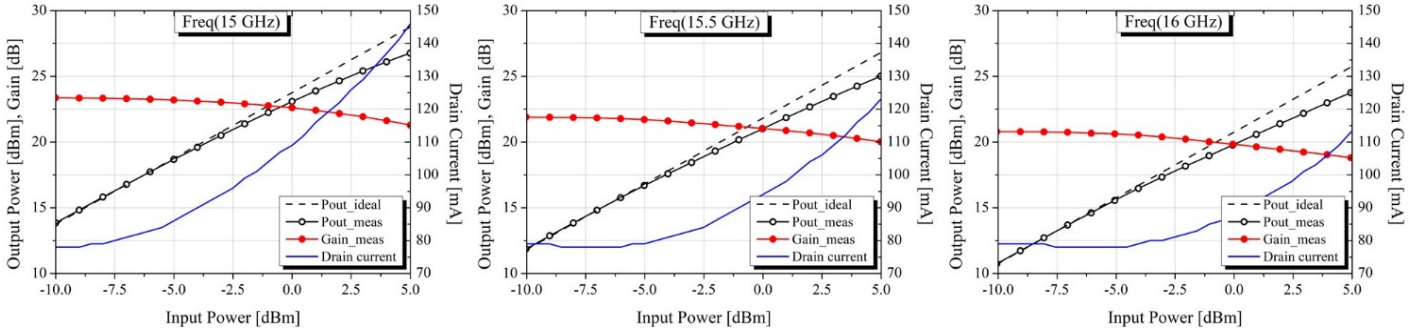

(a) (b) (c)

Fig. 10. Output power and power gain of the low-noise amplifier MMIC with an increase in input power: (a) at 15 GHz, (b) at 15.5 GHz, and (c) at 16 GHz.

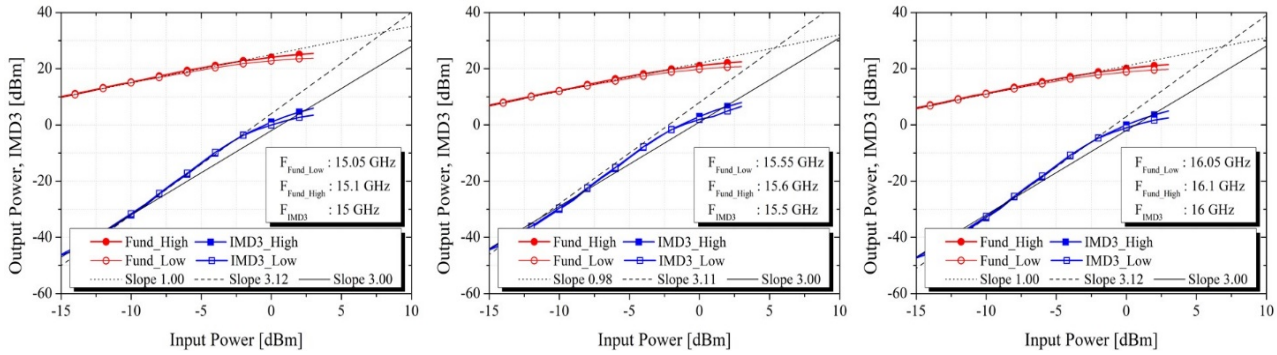

(a) (b) (c)

Fig. 11. Measured third-order intermodulation distortion product (IMD_3) of the low-noise amplifier MMIC with two-tone signal input ($f_{IMD3} = 2f_{Low} - f_{High}$, $\Delta f = 50$ MHz): (a) at 15 GHz, (b) at 15.5 GHz, and (c) at 16 GHz.

Table 3. Comparison of the proposed amplifier with previously published Ku-band low-noise amplifier MMICs

Study	Frequency (GHz)	Gain (dB)	Noise figure (dB)	Input return loss (dB)	$P_{1dB,in}$ (dBm)	$P_{1dB,out}$ (dBm)	OIP_3 (dBm)	DC voltage (V)/ current (mA)	Size (mm^2)	Process
Guo & Yao [13]	14−18	≥18	2.4	≥7	N/A	N/A	N/A	10 / 76	2.2	GaN HEMT
Resca et al. [14]	12.8−14.8	≥20	1.85	≥9	13.8	25	N/A	10 / 2	8.0	GaN HEMT
Suijker et al. [15]	14	≥19.8	1.7	≥6	N/A	≥28	N/A	10 / 72	6.0	GaN HEMT
Laxmi et al. [16]	16−18	30	≤1.3	10	N/A	10	20	3 / 85	4.5	GaAs pHEMT
Kong et al. [17]	14.7−17.3	21.3	1.46	N/A	−10.8	8.05	N/A	4 / 5	1.5	GaAs pHEMT
Arican et al. [18]	14.5−14.8	≥18.8	≤ 0.9	≥12	−11.5	4.8	N/A	1.2 / 30	6.3	GaAs mHEMT
Gupta et al. [19]*	15.5−17.5	25	2.5	≥12	N/A	N/A	N/A	7 / 45	6.3	GaN HEMT
Mayock et al. [20]	5.5−18	≥12	≤4.5	≥10	−2*	10	N/A	12 / 60	7	GaN HEMT
This work	15−16	21.3−22.6	1.7−1.8	19.6−21	0.4−1.5	24.3	27.6−33.3	20 / 84	1.9	GaN HEMT

N/A=not available. *estimated results.

References

[1] I. J. Bahl, *Fundamentals of RF and Microwave Transistor Amplifiers*. Hoboken, NJ: John Wiley & Sons, 2009.

[2] M. Thorsell, M. Fagerlind, K. Andersson, N. Billstrom, and N. Rorsman, "An X-band AlGaN/GaN MMIC receiver front-end," *IEEE Microwave and Wireless Components Letters*, vol. 20, no. 1, pp. 55-57, 2010. https://doi.org/10.1109/LMWC.2009.2035968

[3] C. V. Rao, D. K. Ghodgaonkar, and N. Sharma, "GaAs MMIC low noise amplifier with integrated high-power absorptive receive protection switch," *IEEE Microwave and Wireless Components Letters*, vol. 28, no. 12, pp. 1128-1130, 2018. https://doi.org/10.1109/LMWC.2018.2877148

[4] A. Barigelli, W. Ciccognani, S. Colangeli, P. Colantonio, M. Feudale, F. Giannini, et al., "Development of GaN based MMIC for next generation X-band space SAR T/R module," in *Proceedings of 2012 7th European Microwave Integrated Circuit Conference*, Amsterdam, Netherlands, 2012, pp. 369-372.

[5] S. D'Angelo, A. Biondi, F. Scappaviva, D. Resca, and V. A. Monaco, "A GaN MMIC chipset suitable for integration in future X-band spaceborne radar T/R module frontends," in *Proceedings of 2016 21st International Conference on Microwave, Radar and Wireless Communications (MIKON)*, Krakow, Poland, 2016, pp. 1-4. https://doi.org/10.1109/MIKON.2016.7492014

[6] K. K. Ryu, K. B. Ahn, and S. C. Kim, "A 4W GaAs power amplifier MMIC for Ku-band satellite communication applications," *JSTS: Journal of Semiconductor Technology and Science*, vol. 15, no. 4, pp. 501-505, 2015. https://doi.org/10.5573/JSTS.2015.15.4.501

[7] LearnElectronicWithMe, "Gallium arsenide devices, advantages, energy band gap," 2020 [Online]. Available: https://www.learnelectronicswithme.com/2020/09/gallium-arsenide-devices-advantages.html.

[8] M. P. Lee, S. Kim, S. J. Hong, and D. W. Kim, "Compact 20-W GaN internally matched power amplifier for 2.5 GHz to 6 GHz jammer systems," *Micromachines*, vol. 11, no. 4, article no. 375, 2020. https://doi.org/10.3390/mi11040375

[9] C. T. Fu, C. N. Kuo, and S. S. Taylor, "Low-noise amplifier design with dual reactive feedback for broadband simultaneous noise and impedance matching," *IEEE Transactions on Microwave Theory and Techniques*, vol. 58, no. 4, pp. 795-806, 2010. https://doi.org/10.1109/TMTT.2010.2041570

[10] H. W. Sung, S. H. Han, S. I. Kim, H. K. Ahn, J. W. Lim, and D. W. Kim, "C-band GaN dual-feedback low-noise amplifier MMIC with high-input power robustness," *Journal of Electromagnetic Engineering and Science*, vol. 22, no. 6, pp. 678-685, 2022. https://doi.org/10.26866/jees.2022.6.r.137

[11] O. Ceylan, L. Marco, and S. Pires, "Refine biasing networks for high PA low-frequency stability," *Microwaves and RF*, vol. 57, no. 4, pp. 52-56, 2018.

[12] K. Barkley, "Two-tone IMD measurement techniques," *RF Design*, vol. 24, pp. 36-52, 2001.

[13] F. Guo and Z. Yao, "Design of a Ku-band AlGaN/GaN low noise amplifier," in *Proceedings of 2014 3rd Asia-Pacific Conference on Antennas and Propagation*, Harbin, China, 2014, pp. 1406-1408. https://doi.org/10.1109/APCAP.2014.6992789

[14] D. Resca, F. Scappaviva, C. Florian, S. Rochette, J. L. Muraro, V. di Giacomo Brunel, C. Chang, and D. Baglieri, "A robust Ku-band low noise amplifier using an industrial 0.25-μm AlGaN/GaN on SiC process," in *Proceedings of 2013 European Microwave Conference*, Nuremberg, Germany, pp. 1467-1470. https://doi.org/10.23919/EuMC.2013.6686945

[15] E. M. Suijker, M. Rodenburg, J. A. Hoogland, M. Van Heijningen, M. Seelmann-Eggebert, R. Quay, P. Bruckner, and F. E. van Vliet, "Robust AlGaN/GaN low noise amplifier MMICs for C-, Ku-and Ka-band space applications," in *Proceedings of 2009 Annual IEEE Compound Semiconductor Integrated Circuit Symposium*, Greensboro, NC, USA, 2009, pp. 1-4. https://doi.org/10.1109/csics.2009.5315640

[16] M. Laxmi, S. Karthik, and H. Nagaveni, "High gain and low noise MMIC amplifier for Ku band applications," in *Proceedings of 2021 IEEE MTT-S International Microwave and RF Conference (IMARC)*, Kanpur, India, 2021, pp. 1-4. https://doi.org/10.1109/IMaRC49196.2021.9714656

[17] S. Kong, S. Wang, H. D. Lee, B. H. Park, S. Jang, and S. B. Hyun, "A Ku-band cascode low noise amplifier using InGaAs E-mode 0.15-um pHEMT technology," in *Proceedings of 2022 14th Global Symposium on Millimeter-Waves & Terahertz (GSMM)*, Seoul, South Korea, 2022, pp. 32-34. https://doi.org/10.1109/GSMM53818.2022.9792325

[18] G. O. Arican, N. Akcam, and E. Yazgan, "Ku-band MMIC LNA design for space applications," in *Proceedings of 2019 6th International Conference on Electrical and Electronics Engineering (ICEEE)*, Istanbul, Turkey, 2019, pp. 274-278. https://doi.org/10.1109/ICEEE2019.2019.00059

[19] P. Gupta, M. Imran, and M. Mishra, "GaN HEMT based Ku band LNA and SPDT switch for transmit-receive application," in *Proceedings of 2022 IEEE International Conference on Emerging Electronics (ICEE)*, Bangalore, India, 2022, pp. 1-5. https://doi.org/10.1109/ICEE56203.2022.10117990

[20] J. Mayock, P. Deshpande, Q. Sun, D. Palombini, and M. Papi, "Robust GaN limiting LNA for C-Ku band T/R modules," in *Proceedings of 2019 PhotonIcs & Electromagnetics Research Symposium-Spring (PIERS-Spring)*, Rome, Italy, 2019, pp. 1688-1694. https://doi.org/10.1109/PIERS-Spring46901.2019.9017459

Seong-Hee Han
https://orcid.org/0000-0002-5103-9074

received his B.S. and M.S. degrees in radio science and engineering from Chungnam National University, Daejeon, Republic of Korea, in 2021 and 2023, respectively. He is currently a Ph.D. candidate at the same university. His research interests include 3D printing techniques for microwave components, as well as GaAs pHEMT or GaN HEMT monolithic integrated circuits for microwave, millimeter-wave, and sub-THz front-end applications.

Dong-Wook Kim
https://orcid.org/0000-0003-1913-4714

received his B.S. degree in electronic communications from Hanyang University, Seoul, Republic of Korea, in 1990, and his M.S. and Ph.D. degrees in electrical engineering from Korea Advanced Institute of Science and Technology (KAIST), Daejeon, Republic of Korea, in 1992 and 1996, respectively. In 1996, he joined LG Electronics Research Center in Seoul, Republic of Korea, where he developed high-power III–V semiconductor devices and monolithic microwave integrated circuits. From 2000 to 2002, as a director of the R&D center in Telephus Inc., he led research and development teams in creating RF-integrated passive devices on a thick oxidized Si substrate and their resultant applications. From 2002 to 2004, he was involved in the development of wireless security systems as a team leader at S1 Corporation, a Samsung Group company. In 2004, he joined the faculty of Chungnam National University, Daejeon, Republic of Korea. In 2009, he joined Electronics and Telecommunications Research Institute (ETRI) as an invited researcher. He joined the University of California at San Diego, La Jolla, in 2010 as a visiting scholar. Furthermore, he was the director of the Center for Information and Communication at Chungnam National University from 2016 to 2018, and is currently a full professor and the director of the Radiowave and Electrical Engineering Research Center at the university. He has been a senior member of the IEEE since 2017. His research interests are GaAs- and GaN-based MMICs, internally matched power amplifiers, and microwave/millimeter-wave embedded modules, including miniaturized radar/sensor modules and ultra-wideband high-power modules.